

Size Effects on the Cross-Plane Thermal Conductivity of Transparent Conducting Indium Tin Oxide (ITO) and Fluorine Tin Oxide (FTO) Thin Films

David H. Olson, Christina M. Rost, John T. Gaskins, Chester J. Szejewski, Jeffrey L. Braun, Patrick E. Hopkins

Abstract—Visibly transparent and electrically conductive oxides are attractive for a wide array of applications. Indium tin oxide (ITO) and fluorine tin oxide (FTO) are a subset of the larger transparent conducting oxide family, and possess transmittance in the visible spectrum as well as high electrical conductivity. Even though their unique optical and electrical properties have been thoroughly examined, the thermal transport properties, namely thermal conductivity in the cross-plane direction, have received much less attention. In this paper, using a series of ITO and FTO thin films comprising a range of thicknesses and grain sizes, we characterize the cross-plane thermal conductivity using time-domain thermoreflectance. We determine the heat capacity of the FTO films from simultaneous measurements of volumetric heat capacity and thermal conductivity on an ~396 nm thick FTO film. We show that size effects have a considerable influence on the thermal conductivity from both the perspective of grain boundary and thin film scattering.

Index Terms—transparent conducting oxide, ITO, FTO, thin film, heat capacity, thermal conductivity, TDTR

I. INTRODUCTION

DUE to their transparency in the visible spectrum and electrically conductive nature, transparent conducting oxides (TCOs) have been employed for use in a wide array of technologies, architectural glass applications, flat-panel displays, and organic photovoltaic devices [1; 2; 3]. The leading TCO for photovoltaic and flat-panel display applications is a solid solution of indium oxide and tin oxide, often referred to as indium tin oxide (ITO). While the TCO fluorine tin oxide (FTO) is not as widely used as ITO, its energy efficiency

lends itself to various architectural applications. This is due to FTO’s low emissivity of 0.2 [4], making it less susceptible to radiative heat loss. ITO-coated glass is commonly used as the hole-injecting electrode in polymer light emitting diodes (LEDs) [5; 6]. However, the use of ITO has presented several key problems for energy conversion. Reports in the literature have exemplified diffusion of indium into polymer LEDs [7] and high surface roughnesses of ITO [8], which contribute to undermining carrier-injection characteristics of the electrode. Current heating in polymer LEDs has been shown to elevate temperatures up to 60 °C, limiting maximum attainable efficiencies in devices [9]. Attempts have been made to examine the influence of the electrode heat sink by employing a thermally conductive substrate [10], however no robust examination has been performed on heat dissipation mechanisms in the ITO or FTO electrodes. As thermal conductivities of devices in their thin film form can be drastically reduced compared to their bulk counterparts due to scattering of carriers at the boundary between adjacent layers, their mechanisms of heat dissipation can also be drastically altered. Thus, a further understanding of the influence of film thickness and grain size on thermal conductivity in these TCOs is crucial for mitigating the build up of heat, ultimately improving device performance.

While the electrical and optical properties of ITO and FTO in their thin film form have been thoroughly studied [11; 12; 13; 14; 15; 16], the associated thermal properties have received less attention. To this point, Refs. [17; 18] have

This paper was submitted for review on December 8, 2017. The work performed was supported by the Virginia Space Grant Consortium and the Army Research Office under grant W911NF-16-1-0320.

D. H. Olson (e-mail: dho8rd@virginia.edu), C. J. Szejewski (e-mail: cjs5bx@virginia.edu), and J. L. Braun (e-mail: jlb3gb@virginia.edu) are PhD candidates under the ExSiTE Laboratory at the Department of Mechanical Engineering at the University of Virginia, Charlottesville, VA 22904, USA.

C. M. Rost is a Postdoctoral Associate of the ExSiTE Laboratory at the Department of Mechanical and Aerospace Engineering at the University of Virginia, Charlottesville, VA 22904, USA (e-mail: cmr4fb@virginia.edu).

J. T. Gaskins is a Senior Scientist at the ExSiTE Laboratory at the Department of Mechanical and Aerospace Engineering at the University of Virginia, Charlottesville, VA 22904, USA (e-mail: jtg2e@virginia.edu).

P. E. Hopkins is the Principal Investigator of the ExSiTE Laboratory at the Department of Mechanical and Aerospace Engineering at the University of Virginia, Charlottesville, VA 22904, USA (e-mail: peh4v@virginia.edu), and is an Associate Professor in the Department of Mechanical and Aerospace Engineering, Department of Materials Science and Engineering, and Department of Physics at the University of Virginia.

TABLE I
SHEET RESISTANCES, FILM THICKNESSES, AND GRAIN SIZES OF ITO AND FTO THIN FILMS

Sample ID	Sheet Resistance (Ohms/sq)	Thin Film Thickness (nm)	Grain Size (nm)
40IN	7.79 ± 0.15	205.0 ± 9.7	37.3 ± 1.1
60IN	22.81 ± 0.46	80.6 ± 11.1	27.0 ± 0.9
90IN	78.09 ± 5.54	28.8 ± 2.3	28.8 ± 2.3
9FTO	7.59 ± 0.01	709.0 ± 27.5	138.9 ± 9.7
11FTO	9.90 ± 0.06	467.6 ± 36.1	102.2 ± 5.1
14FTO	13.33 ± 0.16	396.2 ± 13.8	81.2 ± 6.1

examined the thermal conductivity of ITO thin films, but due to the limited range of film thicknesses examined in these studies, no significant film thickness dependence was shown. Despite the analysis of the thermal properties of ITO, values for the cross-plane thermal conductivity of FTO do not exist in the literature, to the best of our knowledge. The advantage of FTO over ITO in polymer LEDs [19] and solar cells [20] suggest the need for a better understanding of the material’s mechanisms of thermal conduction. Therefore, in this paper, we report on the cross-plane thermal conductivity of a series of ITO and FTO thin films with varying thicknesses and grain sizes, demonstrating the role of size effects in these TCOs.

II. METHODS

ITO and FTO thin films were purchased from Delta Technologies Ltd. Sample ID’s from the manufacturer are provided in Table I. ITO thin films were deposited using a 90% In₂O₃ and 10% SnO₂ target via physical vapor deposition (PVD). Information regarding the deposition method for the FTO films was not available. The ITO films were deposited on Corning alkaline earth boro-aluminosilicate glass, while the FTO thin films were deposited on float glass. Thickness

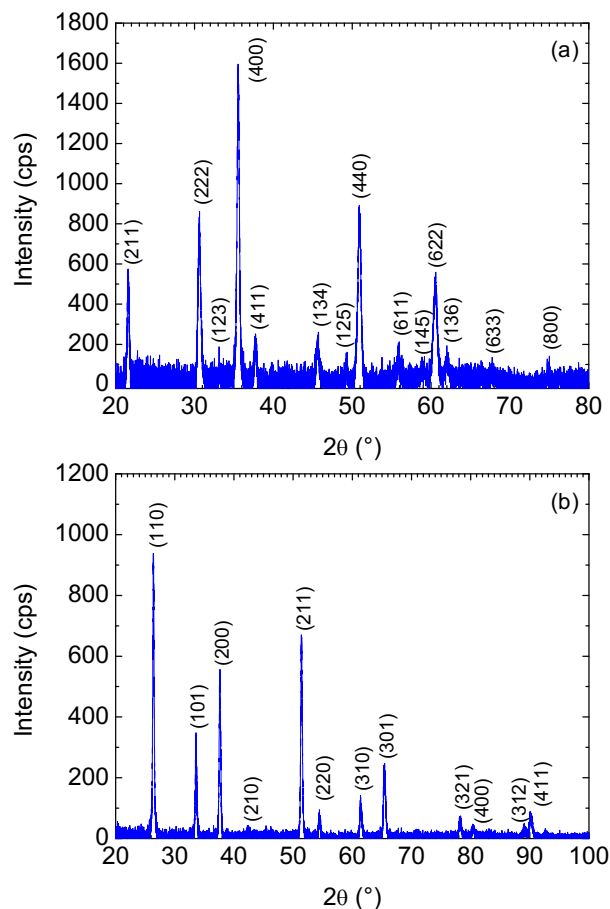


Fig. 1. Background subtracted x-ray diffractograms for (a) 40IN and (b) 9FTO.

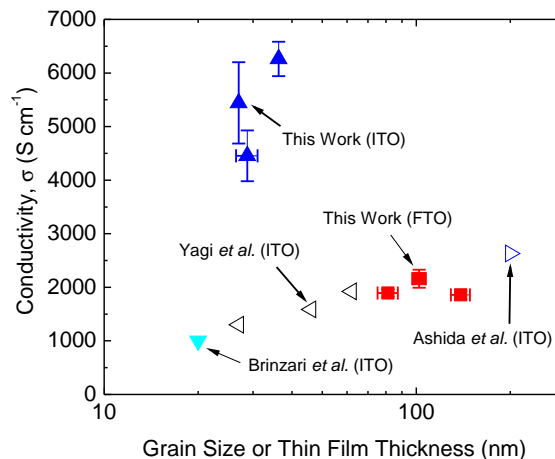


Fig. 2. Electrical conductivity of ITO and FTO as a function of film thickness and grain size, with data from Refs. [17; 18; 23] included. Filled symbols are samples where grain size is the limiting length scale, whereas open symbols are those where the film thickness is the limiting length scale. Note: the data from Ashida *et al.* [18] is with an O₂ flow rate of 0%, while that of Brinzari *et al.* [23] is their assumed electrical conductivity for modeling purposes.

measurements were performed via cross-sectional scanning electron microscopy (SEM), while grain size measurements were performed on plan-view images using the Heyn lineal intercept method [21]. Sheet resistance was determined using a Keithly 2612A sourcemeter combined with a four point probe system. A summary of the sheet resistances, film thicknesses, and grain sizes are listed in Table I. Note: due to the thinness of the film, the grain size was not recoverable for the 90IN sample, and we therefore consider its thickness as the grain size. Considering its thinness, we feel that this is a plausible assumption. ITO and FTO film structures were determined via x-ray diffraction (XRD) using a Rigaku SmartLab diffractometer. Example x-ray diffractograms of ITO and FTO films are shown in Fig. 1. We deposit a nominally 80 nm thick aluminum film onto the surface of the ITO and FTO films to act as a transducer layer for thermal measurements via time-domain thermoreflectance (TDTR). The thickness of the transducer film was verified with profilometry, which agrees within 5% of the nominal thickness as registered by the electron-beam evaporator and picosecond acoustics [22].

TDTR is an optical pump-probe technique that monitors the temperature-induced change in reflectivity of a sample surface (i.e., thermoreflectivity [24; 25; 26; 27]) as a function of time to determine the thermal properties of thin film systems [28]. TDTR utilizes a sub-picosecond pulsed laser (Ti:Sapphire oscillator), which outputs a train of laser pulses centered at 800 nm with a repetition rate of 80 MHz and bandwidth of 10.5 nm. The output is split into two paths, a frequency doubled (400 nm) and electro-optically modulated pump, and a time-delayed (via a mechanical delay stage) probe. This modulated heating event, f , from the pump can be tuned between 0.1 and 10 MHz, allowing for sensitivity to different thermophysical parameters, which will be discussed further below. The pump

and probe beams are focused through an objective onto the surface of the sample, yielding pump and probe $1/e^2$ radii of 17 and 7 μm , respectively, with a 5x objective (Mitutoyo Part No. 378-803-3). The reflected probe beam is monitored via a Si photodiode, and further processed through lock-in amplification to monitor the in-phase and out-of-phase voltages generated in the probe from the modulated heating event. A radially symmetric, multilayer thermal model is used to fit the probe thermorefectivity decay as a function of time, allowing us to extract thermophysical properties of interest. It should be noted that we restrict pump and probe incident laser powers to ~ 5 and ~ 4 mW, respectively, in order to minimize steady-state heating induced by the average absorbed power from the pump and probe [29; 30]. A more robust description of TDTR analyses is found in Refs. [31; 32; 33]. We exploit the fact that a change in pump modulation frequency, and its associated change in thermal penetration depth characterized by

$$\delta_{thermal} = \sqrt{\frac{\kappa_{sub}}{\pi C_{sub} f}}, \quad (1)$$

offers varying sensitivity of the measurement to parameters of interest [34], and is dependent on the thermal conductivity and volumetric heat capacity of the substrate, κ_{sub} and C_{sub} , respectively. This change in sensitivity with varying modulation frequency allows us to simultaneously determine both thermal conductivity, κ , and volumetric heat capacity, C of the intermediate film in 14FTO sample. There are no reports in the literature regarding the volumetric heat capacity of ITO, and thus we assumed the value of (In_2O_3 2.58 MJ m^{-3} K^{-1} [35]) in the analysis of the thermal conductivity of ITO thin films. The literature value of In_2O_3 was also assumed in the analysis of Refs. [17; 18]. While simultaneous measurements of κ and C of ITO films would have been ideal, limitations in film thickness ultimately undermined our sensitivity to these two parameters in our measurements. To ensure our results take uncertainty of the heat capacity of ITO into account, we analyze our data with 10% error in heat capacity, which presents as an additional term in our error analysis.

III. DISCUSSION

XRD was used to confirm the phase of our deposited thin films. Figure 1 shows the background subtracted diffractograms acquired for the thickest films of ITO and FTO, as the thinner films proved too thin for reliable measurement. ITO, shown in Fig. 1(a), exhibits a cubic unit cell of space group Ia-3 (space group number: 206). FTO, shown in Fig. 1(b), exhibits a tetragonal unit cell of space group P42/mnm (space group number: 136). Using the angular position of the peaks, it was determined that the lattice parameters of ITO are $a = 10.4$ \AA and FTO are $a = 4.8$ \AA and $c = 3.4$ \AA , respectively. Both samples are highly crystalline in nature, as evidenced by the sharp, easily discernable peaks in their diffractograms. The crystal structures and respective lattice parameters are found to be consistent with the literature [36; 15; 12; 37]. Amorphous materials have been shown to have significantly reduced thermal conductivities compared to their crystalline

counterparts, and thus the confirmation of the crystalline nature of these samples is paramount for understanding the underlying mechanisms of heat transfer. The thermal conductivity of amorphous silicon thin films, for example, have been shown to be two orders of magnitude smaller than their bulk, crystalline counterparts [38; 39]. This is due to the fact that the length scales that govern heat propagation are on the order of the bond length in amorphous systems, hence the reduced thermal conductivity. However, these films are still prone to influences of extrinsic geometric features, such as the boundaries of the thin film itself. Due to the longer intrinsic length scales found in crystalline systems, these systems are more heavily influenced by extrinsic features, such as film thickness or grain size.

We compute the electrical conductivity of our thin films using thickness and sheet resistance values for each film as shown in Table I. These values are displayed in Fig. 2, alongside other values found in the literature [17; 18]. Note: the measurements were in Refs. [17] and [18] were performed via the van der Pauw and four point probe methods, respectively, and thus represent electronic conduction in the in-plane direction. It is interesting to note that the electrical conductivity of our ITO samples increases with grain size. Similar trends were observed in the work of Ashida *et al.* [18], although the values for electrical conductivity reported were much smaller than ours. This is possibly due to the fact that the films in Ashida *et al.* [18] were deposited with varying oxygen flow rates and then post-annealed at 200 $^\circ\text{C}$ in an Ar atmosphere for 1 hour. In both cases, however, a 90% In_2O_3 and 10% SnO_2 target was used, suggesting the difference in electrical conductivity is most likely due to fabrication conditions. As the XRD in Ref. [18] is very similar to that of ours, we expect to have thin films of similar polycrystalline morphology. We observe no grain size dependence in FTO films; however, considering the large grain sizes present in these systems, this is not unexpected. Despite having much larger grain sizes than the ITO films, these films are clearly less conductive than their ITO counterparts.

As mentioned previously, changing the modulation frequency, f , of the pump causes an alteration of the thermal penetration depth [29]. Additionally, changing the thermal penetration depth alters the sensitivity to parameters such as volumetric heat capacity or thermal conductivity. Figure 3(a) shows a sensitivity analysis for the thermal conductivity and volumetric heat capacity of 14FTO at modulation frequencies of 0.5 and 10 MHz. At a given frequency, we are simultaneously sensitive to both the thermal conductivity of the thin film as well as its volumetric heat capacity. Altering our sensitivity to κ and C by changing modulation frequencies allows us to simultaneously determine both thermophysical properties of the thin films [34].

Using this concept, we performed TDTR measurements with pump modulation frequencies of 0.5, 2.4, 4.3, 6.2, 8.1, and 10 MHz on three different locations of the FTO samples. We then fit for thermal conductivity in the model while stepping through values of volumetric heat capacity for the 14FTO sample; example TDTR data and best fit model at 10 MHz is shown in Fig. 3(b). This κ - C analysis is shown in Fig.

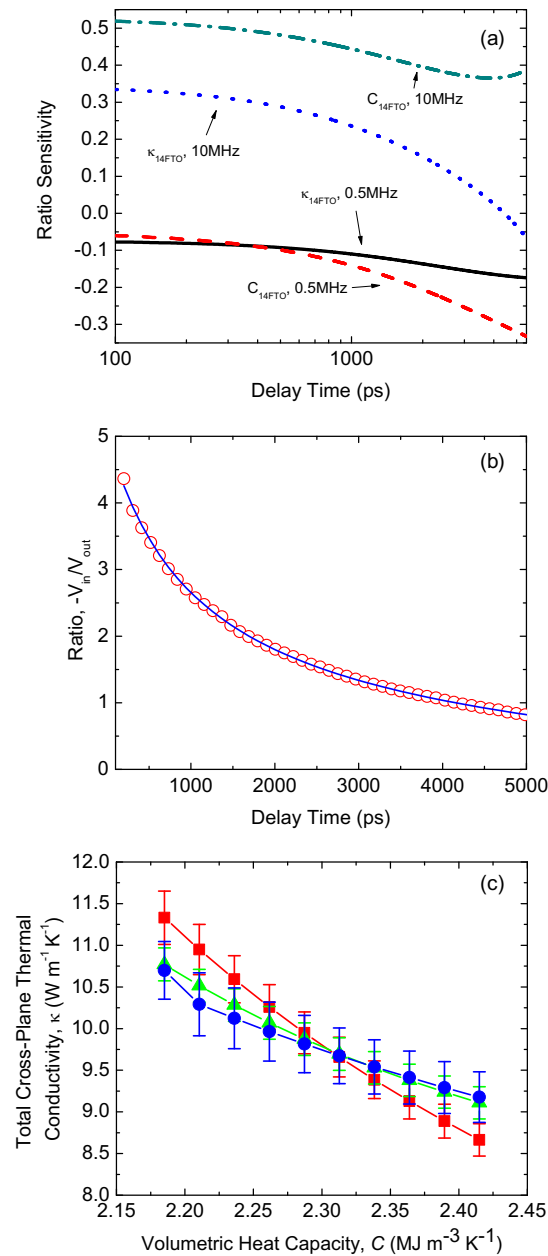


Fig. 3. (a) Sensitivity to thermal conductivity, κ and volumetric heat capacity, C at 0.5 and 10 MHz modulation frequencies in 14FTO. For these calculations, we use $C_{14FTO} = 2.32 MJ m^{-3} K^{-1}$, $d_{14FTO} = 396.2 nm$, and $\kappa_{14FTO} = 9.7 W m^{-1} K^{-1}$. (b) TDTR data and the best fit for 14FTO. (c) The κ - C diagram of 14FTO; only 3 of the 6 frequencies used in this analysis are shown for clarity. The red squares, green triangles, and blue circles represent data at modulation frequencies of 0.5, 4.3, and 10 MHz, respectively, and the intersection between the lines is the volumetric heat capacity and thermal conductivity of the sample.

3(c) for 14FTO, which shows the results of this TDTR analysis at three different frequencies (0.5, 4.5, and 10 MHz). In this analysis, multiple pairs of κ and C are used to satisfy a best-fit in the experimental data for that particular frequency. The crossover point between modulation frequencies represents the values of thermal conductivity and volumetric heat capacity

that provide a similar best fit for the same values at all three modulation frequencies in the 14FTO sample. From this, we take the volumetric heat capacity of $2.32 MJ m^{-3} K^{-1}$ for FTO from the crossover point, which we also used to fit for thermal conductivity values in the 9FTO and 11FTO samples. Note, we do not expect size effects in the heat capacity for FTO films of this thickness since the heat capacity is governed by the phononic density of states, which does not exhibit size effects until extrinsic geometric features approach the length scale of the phonon wavelength [40]. However, the thermal conductivity can be influenced by these extrinsic size effects when the carrier mean free paths approach the size of extrinsic geometric features. Thus, the thermal conductivity must be measured on all samples regardless of the thickness to determine this size effect influence.

The thermal conductivity of electrons and phonons can be approximated as $\kappa = Cv^2\tau/3$, where v and τ are the thermal carrier velocities and relaxation times, respectively [15]. The latter is driven by the scattering events of the thermal carriers that govern momentum and energy exchange. As discussed earlier, for these film thicknesses and grain sizes, we can assume that the heat capacities and velocities are relatively constant. Thus, the most influential variable in the expression for κ is the scattering time τ . Under Matthiessen's rule, the scattering rate is dependent on a variety of interactions, both intrinsic and extrinsic to the material [40]. When the film thicknesses of ITO and FTO approach intrinsic mean free paths, then the total mean free path in each film, and hence the total relaxation time, will be reduced. Thus, we attribute differences in observed thermal conductivities within ITO and FTO sample sets to grain and thin film boundary scattering.

The total thermal conductivity measured from TDTR in ITO and FTO is plotted as a function of thin film thickness in Fig. 4(a) and grain size in Fig. 4(b). Specifically, we measure the thermal conductivities to be 1.38 ± 0.53 , 3.50 ± 0.91 , 6.52 ± 1.04 , $W m^{-1} K^{-1}$ for 90IN, 60IN, and 40IN, respectively, and 9.70 ± 0.47 , 10.74 ± 1.05 , $15.18 \pm 0.84 W m^{-1} K^{-1}$ for 14FTO, 11FTO, and 9FTO, respectively. The uncertainties for our results account for variation from spot-to-spot in our measurements as well as uncertainties in the heat capacities and Al transducer thicknesses in each sample. Included in the figure are the results from Refs. [17; 18; 23] for ITO thin films. In general, one sees that as either the grain size or thin film thickness decreases, there is an associated decrease in the thermal conductivity. Regarding Fig. 4(a), our measured thermal conductivity for 40IN are in good agreement with that of Ashida *et al.* [18], who measured a film of similar thickness. There is, however, a discrepancy between our measured values and those of Yagi *et al.* [17]. Even though the ITO film thicknesses in Yagi *et al.* [17] were similar to ours (27, 46, and 62 nm), they show no dependence of κ on film thickness, measuring a value of $3.2 W m^{-1} K^{-1}$ by simultaneously solving the heat equation for the heat diffusion time of their Mo/ITO/Mo films for two sets of data. We represent their data on the plot by averaging the three film thicknesses, where the uncertainty is the standard deviation of the three samples. The constant thermal conductivity as a function of film thickness is also due to the fact that the films in Ref. [17] are amorphous,

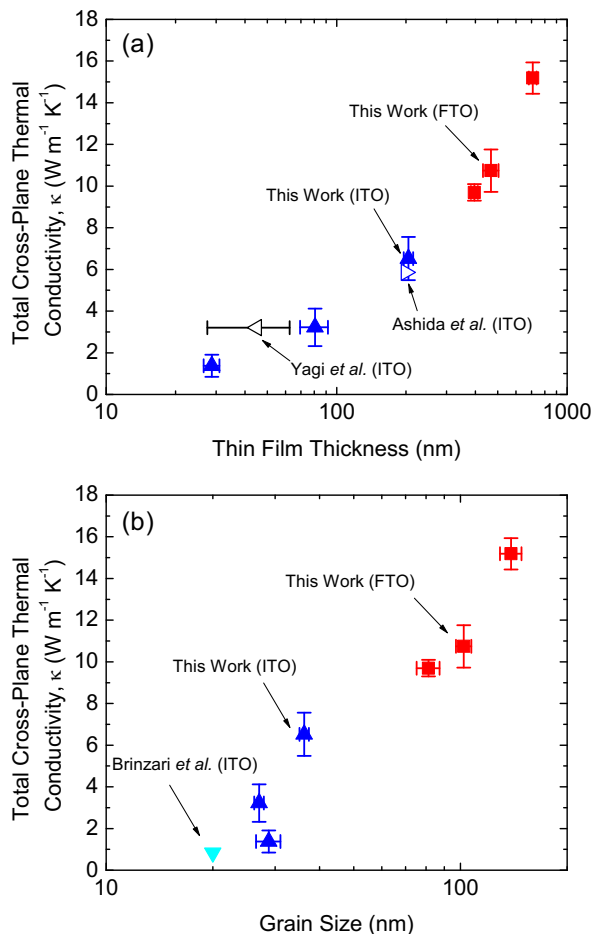


Fig. 4. Total thermal conductivity in the cross-plane direction as a function of (a) film thickness and (b) grain size in ITO and FTO thin films. Included are data from Refs. [17; 18; 23]. Note: the data from Brinzari *et al.* [23] is for a film doped with 5% Sn, while the data from Ashida *et al.* [18] is with an O_2 flow rate of 0%. The error bars in Yagi *et al.*'s measurement comprise three thin films with thicknesses of 27, 46, and 62 nm. Because a single value of thermal conductivity was measured for these three films, the error bar is the standard deviation of the three film thicknesses.

hence the constant thermal conductivity observed between the three films and the discrepancy from our crystalline systems.

In a similar manner, Brinzari *et al.* [23] examined the thermal conductivity of ITO thin films using the laser flash technique, a transient technique that directly measures the thermal diffusivity of samples [41]. This value is presented in Fig. 4(b). When grain sizes become significantly smaller than the film thickness, heat carriers scatter at these boundaries more so than boundaries of the thin film. Indeed, materials with nanoscale grains are known to possess reduced thermal conductivities [42; 43]. In this manner, the limiting length scale in Brinzari *et al.*'s [23] work is not the thickness of the film, but rather the average grain size, and thus it is understandable that the values reported in Ref. [23] are lower than that of this work. The values reported in Ref. [23] are also lower than those of Refs. [17; 18], the reasons for which

could be numerous. The measured thermal conductivity in Brinzari *et al.*'s work is influenced by the thermal resistances of the crystalline solid and interfacial resistance at the grain boundaries that have average spacing on the order of 10's of nanometers, which implies the low thermal conductivity is due to grain boundary scattering. Additionally, differences in the electronic contribution to thermal conductivity can drastically alter the efficiency of heat conduction in these materials, as the total thermal conductivity is the sum of both phononic and electronic contributions. Considering their assumed electrical conductivity was lower than all of those reported in Ref. [17], this is not unreasonable. Thus, a reduction in electronic conductivity combined with a phonon thermal conductivity reduction due to grain boundary scattering has the potential to reduce the thermal conductivity of ITO thin films below the amorphous limit [44].

Despite the size effects on thermal conductivity exhibited in both ITO and FTO thin films, only ITO thin films exhibited size effects on the in-plane electrical conductivity. A direct and quantitative comparison of electronic size effects from our in-plane electrical conductivity results in Fig. 2 to the cross-plane thermal conductivity is not possible. In the ITO films, however, we can not rule out that size effects on the electronic contribution to thermal conductivity could be influencing our measurements. The electrical conductivities of the FTO films are size-independent, suggesting that size effects on the cross-plane thermal conductivity are primarily driven by grain boundary scattering, and not electronic size effects. Given that all of the measured grain sizes in FTO are larger than those of the ITO films studied in this work, this seems like a plausible speculation. We are not aware of any prior works reporting on the thermal conductivity of FTO thin films, let alone size effects impacting phonon transport in these systems and, thus, these results should provide critical insight into the design of electronic and energy conversion devices reliant on FTO as the TCO.

IV. CONCLUSION

We have shown that TCO thin films, namely ITO and FTO, exhibit size effects on thermal conductivity in the cross-plane direction. Thermal conductivities, determined using TDTR, were found to be proportional to the thin film thickness and grain size in FTO and ITO films. With device heating in polymer LEDs contributing to a reduction in device efficiency, our results should provide crucial insight into device design to mitigate heating. With thicker ITO and FTO thin films having corresponding larger thermal conductivities, their use in polymer LEDs is an obvious substitution for their thinner counterparts. While the cross-plane thermal conductivity of both structures have been investigated in this paper, additional analysis of the thermal conductivities, namely contributions from phononic carriers in the in-plane direction and electronic carriers in the cross-plane direction, are necessary.

ACKNOWLEDGMENT

D. H. Olson would like to thank the Virginia Space Grant Consortium (VSGC) for their continued funding and support.

We also appreciate funding from the Army Research Office, Grant. No. W911NF-16-1-0320. We are also thankful for meaningful discussions with Jon Ihlefeld.

REFERENCES

- [1] E. Fortunato, D. Ginley, H. Hosono, and D. C. Paine, "Transparent conducting oxides for photovoltaics," *MRS bulletin*, vol. 32, no. 03, pp. 242–247, 2007.
- [2] D. S. Ginley and C. Bright, "Transparent conducting oxides," *Mrs Bulletin*, vol. 25, no. 08, pp. 15–18, 2000.
- [3] B. G. Lewis and D. C. Paine, "Applications and processing of transparent conducting oxides," *Mrs Bulletin*, vol. 25, no. 08, pp. 22–27, 2000.
- [4] H. De Waal and F. Simons, "Tin oxide coatings: Physical properties and applications," *Thin Solid Films*, vol. 77, no. 1-3, pp. 253–258, 1981.
- [5] I. D. Parker, "Carrier tunneling and device characteristics in polymer light-emitting diodes," *Journal of Applied Physics*, vol. 75, no. 3, pp. 1656–1666, 1994.
- [6] W. R. Salaneck and J. L. Brédas, "Conjugated polymer surfaces and interfaces for light-emitting devices," *MRS Bulletin*, vol. 22, no. 6, pp. 46–51, June 1997.
- [7] A. R. Schlattmann, D. W. Floet, A. Hilberer, F. Garten, P. J. M. Smulders, T. M. Klapwijk, and G. Hadziioannou, "Indium contamination from the indium–tin–oxide electrode in polymer lightemitting diodes," *Applied Physics Letters*, vol. 69, no. 12, pp. 1764–1766, 1996. [Online]. Available: <https://doi.org/10.1063/1.117478>
- [8] T. Kugler, Å. Johansson, I. Dalsegg, U. Gelius, and W. Salaneck, "Electronic and chemical structure of conjugated polymer surfaces and interfaces: applications in polymer-based light-emitting devices," *Synthetic metals*, vol. 91, no. 1, pp. 143–146, 1997.
- [9] N. Tessler, N. Harrison, D. Thomas, and R. Friend, "Current heating in polymer light emitting diodes," *Applied Physics Letters*, vol. 73, no. 6, pp. 732–734, 1998.
- [10] S. H. Choi, T. I. Lee, H. K. Baik, H. H. Roh, O. Kwon, and D. hak Suh, "The effect of electrode heat sink in organic-electronic devices," *Applied Physics Letters*, vol. 93, no. 18, p. 183301, 2008. [Online]. Available: <https://doi.org/10.1063/1.3021071>
- [11] N. Balasubramanian and A. Subrahmanyam, "Electrical and optical properties of reactively evaporated indium tin oxide (ito) films-dependence on substrate temperature and tin concentration," *Journal of Physics D: Applied Physics*, vol. 22, no. 1, p. 206, 1989.
- [12] Z. Y. Banyamin, P. J. Kelly, G. West, and J. Boardman, "Electrical and optical properties of fluorine doped tin oxide thin films prepared by magnetron sputtering," *Coatings*, vol. 4, no. 4, pp. 732–746, 2014.
- [13] M. S. Farhan, E. Zalnezhad, A. R. Bushroa, and A. A. D. Sarhan, "Electrical and optical properties of indium-tin oxide (ito) films by ion-assisted deposition (iad) at room temperature," *International Journal of Precision Engineering and Manufacturing*, vol. 14, no. 8, pp. 1465–1469, 2013.
- [14] T. Karasawa and Y. Miyata, "Electrical and optical properties of indium tin oxide thin films deposited on unheated substrates by dc reactive sputtering," *Thin Solid Films*, vol. 223, no. 1, pp. 135–139, 1993.
- [15] H. Kim, C. Gilmore, A. Pique, J. Horwitz, H. Mattoussi, H. Murata, Z. Kafafi, and D. Chrisey, "Electrical, optical, and structural properties of indium–tin–oxide thin films for organic light-emitting devices," *Journal of Applied Physics*, vol. 86, no. 11, pp. 6451–6461, 1999.
- [16] A. Rakhshani, Y. Makdisi, and H. Ramazaniyan, "Electronic and optical properties of fluorine-doped tin oxide films," *Journal of applied physics*, vol. 83, no. 2, pp. 1049–1057, 1998.
- [17] T. Yagi, K. Tamano, Y. Sato, N. Taketoshi, T. Baba, and Y. Shigesato, "Analysis on thermal properties of tin doped indium oxide films by picosecond thermoreflectance measurement," *Journal of Vacuum Science & Technology A: Vacuum, Surfaces, and Films*, vol. 23, no. 4, pp. 1180–1186, 2005.
- [18] T. Ashida, A. Miyamura, N. Oka, Y. Sato, T. Yagi, N. Taketoshi, T. Baba, and Y. Shigesato, "Thermal transport properties of polycrystalline tin-doped indium oxide films," *Journal of applied physics*, vol. 105, no. 7, p. 073709, 2009.
- [19] A. Andersson, N. Johansson, P. Broms, N. Yu, D. Lupo, W. R. Salaneck *et al.*, "Fluorine tin oxide as an alternative to indium tin oxide in polymer leds," *Advanced Materials*, vol. 10, no. 11, pp. 859–863, 1998.
- [20] Q. Qiao, J. Beck, R. Lumpkin, J. Pretko, and J. T. Mcleskey, "A comparison of fluorine tin oxide and indium tin oxide as the transparent electrode for p3ot/tio 2 solar cells," *Solar energy materials and solar cells*, vol. 90, no. 7, pp. 1034–1040, 2006.
- [21] E. Heyn, "Short reports from the metallurgical laboratory of the royal mechanical and testing institute of charlottenburg," *Metallographist*, vol. 5, pp. 37–64, 1903.
- [22] C. Thomsen, H. Maris, and J. Tauc, "Picosecond acoustics as a non-destructive tool for the characterization of very thin films," *Thin Solid Films*, vol. 154, no. 1, pp. 217 – 223, 1987. [Online]. Available: <http://www.sciencedirect.com/science/article/pii/004060908790366X>
- [23] V. I. Brinzari, A. I. Cocemasov, D. L. Nika, and G. S. Korotcenkov, "Ultra-low thermal conductivity of nanogranular indium tin oxide films deposited by spray pyrolysis," *Applied Physics Letters*, vol. 110, no. 7, p. 071904, 2017.
- [24] P. E. Hopkins, "Effects of electron-boundary scattering on changes in thermoreflectance in thin metal films undergoing intraband excitations," *Journal of Applied Physics*, vol. 105, no. 9, p. 093517, 2009.
- [25] P. E. Hopkins, "Influence of electron-boundary scattering on thermoreflectance calculations after intra-and interband transitions induced by short-pulsed laser absorption," *Physical Review B*, vol. 81, no. 3, p. 035413, 2010.
- [26] R. Rosei, "Temperature modulation of the optical transitions involving the fermi surface in ag: Theory," *Physical Review B*, vol. 10, no. 2, p. 474, 1974.
- [27] Y. Wang, J. Y. Park, Y. K. Koh, and D. G. Cahill, "Thermoreflectance of metal transducers for time-domain thermoreflectance," *Journal of Applied Physics*, vol. 108,

- no. 4, p. 043507, 2010.
- [28] D. G. Cahill, P. V. Braun, G. Chen, D. R. Clarke, S. Fan, K. E. Goodson, P. Keblinski, W. P. King, G. D. Mahan, A. Majumdar *et al.*, “Nanoscale thermal transport. ii. 2003–2012,” *Applied Physics Reviews*, vol. 1, no. 1, p. 011305, 2014.
- [29] J. L. Braun and P. E. Hopkins, “Upper limit to the thermal penetration depth during modulated heating of multilayer thin films with pulsed and continuous wave lasers: A numerical study,” *Journal of Applied Physics*, vol. 121, no. 175107, 2017.
- [30] J. L. Braun, C. J. Szejewski, A. Giri, and P. E. Hopkins, “On the steady-state temperature rise during laser heating of multilayer thin films in optical pump-probe techniques,” *to appear in Journal of Heat Transfer*, Preprint.
- [31] D. G. Cahill, “Analysis of heat flow in layered structures for time-domain thermoreflectance,” *Review of scientific instruments*, vol. 75, no. 12, pp. 5119–5122, 2004.
- [32] P. E. Hopkins, J. R. Serrano, L. M. Phinney, S. P. Kearney, T. W. Grasser, and C. T. Harris, “Criteria for cross-plane dominated thermal transport in multilayer thin film systems during modulated laser heating,” *Journal of Heat Transfer*, vol. 132, no. 8, p. 081302, 2010.
- [33] A. J. Schmidt, X. Chen, and G. Chen, “Pulse accumulation, radial heat conduction, and anisotropic thermal conductivity in pump-probe transient thermoreflectance,” *Review of Scientific Instruments*, vol. 79, no. 11, p. 114902, 2008.
- [34] J. Liu, J. Zhu, M. Tian, X. Gu, A. Schmidt, and R. Yang, “Simultaneous measurement of thermal conductivity and heat capacity of bulk and thin film materials using frequency-dependent transient thermoreflectance method,” *Review of Scientific Instruments*, vol. 84, no. 3, p. 034902, 2013.
- [35] I. Barin, “Thermochemical data of pure substances,” *VHC Verlagsgesellschaft mbH*, vol. 271, 1989.
- [36] N. Nadaud, N. Lequeux, M. Nanot, J. Jove, and T. Roisnel, “Structural studies of tin-doped indium oxide (ito) and $\text{In}_4\text{Sn}_3\text{O}_{12}$,” *Journal of Solid State Chemistry*, vol. 135, no. 1, pp. 140–148, 1998.
- [37] W. Z. Samad, M. M. Salleh, A. Shafiee, and M. A. Yarmo, “Structural, optical and electrical properties of fluorine doped tin oxide thin films deposited using inkjet printing technique,” *Sains Malaysiana*, vol. 40, no. 3, pp. 251–257, 2011.
- [38] J. L. Braun, C. H. Baker, A. Giri, M. Elahi, K. Artyushkova, T. E. Beechem, P. M. Norris, Z. C. Leseman, J. T. Gaskins, and P. E. Hopkins, “Size effects on the thermal conductivity of amorphous silicon thin films,” *Physical Review B*, vol. 93, no. 14, p. 140201, 2016.
- [39] C. J. Glassbrenner and G. A. Slack, “Thermal conductivity of silicon and germanium from 3k to the melting point,” *Phys. Rev.*, vol. 134, pp. A1058–A1069, May 1964. [Online]. Available: <https://link.aps.org/doi/10.1103/PhysRev.134.A1058>
- [40] G. Chen, *Nanoscale energy transport and conversion: a parallel treatment of electrons, molecules, phonons, and photons*. Oxford University Press, 2005.
- [41] G. Penco, D. Barni, P. Michelato, and C. Pagani, “Thermal properties measurements using laser flash technique at cryogenic temperature,” in *Particle Accelerator Conference, 2001. PAC 2001. Proceedings of the 2001*, vol. 2. IEEE, 2001, pp. 1231–1233.
- [42] B. M. Foley, H. J. Brown-Shaklee, J. C. Duda, R. Cheaito, B. J. Gibbons, D. Medlin, J. F. Ihlefeld, and P. E. Hopkins, “Thermal conductivity of nano-grained SrTiO_3 thin films,” *Applied Physics Letters*, vol. 101, no. 23, p. 231908, 2012. [Online]. Available: <http://dx.doi.org/10.1063/1.4769448>
- [43] B. F. Donovan, B. M. Foley, J. F. Ihlefeld, J.-P. Maria, and P. E. Hopkins, “Spectral phonon scattering effects on the thermal conductivity of nano-grained barium titanate,” *Applied Physics Letters*, vol. 105, no. 8, p. 082907, 2014. [Online]. Available: <http://dx.doi.org/10.1063/1.4893920>
- [44] D. G. Cahill, “Lower limit to the thermal conductivity of disordered crystals,” *Physical Review B*, vol. 46, no. 10, p. 6131–6140, 1992.



David H. Olson received a B.S. in physics at James Madison University, Harrisonburg, Virginia, in 2016 and is currently pursuing a Ph.D. in mechanical engineering at the University of Virginia, Charlottesville. From 2014 to 2016, he worked at the NanoSynCh Lab at James Madison University, studying the thermoelectric properties of manganese oxide in its powder and thin film forms. In 2016, he joined the ExSiTE Lab at the University of Virginia to study excited carrier dynamics. David is a recipient of the University of Virginia Commonwealth Fellowship in

Engineering, and is currently a VSGC Graduate Research Fellow.



Patrick E. Hopkins is an Associate Professor in the Department of Mechanical and Aerospace Engineering at U.Va. Patrick received his Ph.D. in Mechanical and Aerospace Engineering from University of Virginia in 2008, following a B.S. in Mechanical Engineering and a B.A. in Physics at U.Va. in 2004. He spent 3 years as a Harry S. Truman Postdoctoral Fellow at Sandia National Laboratories in Albuquerque, NM from 2008-2011. Patrick began his faculty appointment at U.Va. in 12/2011 as an Assistant Professor, and was promoted to Associate

Professor with tenure in 8/2015. Patrick is a recipient of the AFOSR and ONR Young Investigator Awards, the ASME Bergles-Rohsenow Young Investigator Award in Heat Transfer, and the Presidential Early Career Award for Scientists and Engineers (PECASE).



Christina Rost graduated with a Ph.D. in Materials Science and Engineering from North Carolina State University in 2016, following both a B.S. and an M.S. in Physics from Indiana University of Pennsylvania. Her Ph.D. focused on the development and characterization of a novel class of oxide systems stabilized through configurational disorder, named "Entropy Stabilized Oxides". Tina is currently a Postdoctoral Research Associate in the ExSITE group, focusing on experimental methods to test thermal properties at extremely high temperatures

and thermal transport in entropy-stabilized oxides, carbides, nitrides and diborides.



John T. Gaskins graduated with his Ph.D. in Mechanical and Aerospace Engineering from the University of Virginia in 2013 following a B.S. in Civil Engineering and an M.E. in Mechanical and Aerospace Engineering. His Ph.D. focused experimental methods and analytical solutions used to determine elastic-plastic properties of sub-micron thin films via indentation testing of microfabricated structures. He is currently a Senior Scientist in the ExSiTE group, focusing on thermal transport in composites at high temperatures and thermal

mitigation of high power, high frequency devices.



Chester J. Szejewski received a B.S. degree in physics from James Madison University, Harrisonburg, Virginia, USA in 2014. He is currently pursuing a PhD in mechanical engineering at University of Virginia, Charlottesville, Virginia, USA. From 2012 to 2014, he worked as a Research Assistant in the NanoSynCh Lab at James Madison University. He joined the ExSiTE Lab at University of Virginia as a Research Assistant in 2014 to study the thermal properties of soft materials



Jeffrey L. Braun received his B.S in Mechanical Engineering from the University of Maryland in 2012. He then worked for two years at Key Technologies and Office of Naval Intelligence before beginning graduate school at U.Va. in the Fall of 2014. He is currently a PhD student in the department of Mechanical and Aerospace Engineering at U.Va. Jeffrey is a recipient of a University of Virginia Jefferson Fellowship and NDSEG Fellowship.